UDC 621.314 https://doi.org/10.20998/2074-272X.2022.5.07

S. Latreche, A. Khenfer, M. Khemliche

Sensors placement for the faults detection and isolation based on bridge linked configuration of photovoltaic array

Introduction. *The photovoltaic market has been increased over the last decade at a remarkable pace even during difficult economic times. Photovoltaic energy production becomes widely used because of its advantages as a renewable and clean energy source. It is eco-friendly, inexhaustible, easy to install, and the manufacturing time is relatively short. Photovoltaic modules have a theoretical lifespan of approximately 20 years. In real-life and for several reasons, some photovoltaic modules start to fail after being used for a period of 8 to 10 years. Therefore, to ensure safe and reliable operation of photovoltaic power plants in a timely manner, a monitoring system must be established in order to detect, isolate and resolve faults. The* ***novelty*** *of the proposed work consists in the development of a new model of sensors placement for faults detection in a photovoltaic system. The fault can be detected accurately after the analysis of changes in measured quantities.* ***Purpose.*** *Analysis of the possibility of the number and the position of the sensors into the strings in function of different faults.* ***Methods.*** *This new method is adapted to the bridge linked configuration. It can detect and locate failure points quickly and accurately by comparing the measured values.* ***Results****. The feasibility of the chosen model is proven by the simulation results under MATLAB/Simulink environment for several types of faults such as short-circuit current, open circuit voltage in the photovoltaic modules, partially and completely shaded cell and module.* References 21, tables 6, figures 7.
Key words: **sensors placement, fault detection and isolation, healthy and faulty operating, photovoltaic field.**

Вступ*. Ринок фотоелектричної енергії зріс за останнє десятиліття неймовірними темпами навіть у складні економічні часи. Виробництво фотоелектричної енергії стає широко використовуваним через його переваги як відновлюваного та чистого джерела енергії. Він екологічно чистий, невичерпний, простий в установці, а час виготовлення відносно короткий. Фотоелектричні модулі мають теоретичний термін служби приблизно 20 років. У реальному житті з кількох причин деякі фотоелектричні модулі починають виходити з ладу після використання протягом 8-10 років. Тому для своєчасного забезпечення безпечної та надійної роботи фотоелектричних електростанцій необхідно створити систему моніторингу для виявлення, локалізації та усунення несправностей.* ***Новизна*** *запропонованої роботи полягає в розробці нової моделі розміщення датчиків для виявлення несправностей у фотоелектричній системі. Несправність можна точно виявити після аналізу змін вимірюваних величин.* ***Мета****. Аналіз можливості кількості та розташування датчиків у рядках залежно від різних несправностей.* ***Методи****. Цей новий метод адаптовано до конфігурації, пов'язаної з мостом. Він може швидко й точно виявляти та локалізувати точки збою, порівнюючи виміряні значення.* ***Результати****. Здійсненність обраної моделі підтверджується результатами моделювання в середовищі MATLAB/Simulink для кількох типів несправностей, таких як струм короткого замикання, напруга холостого ходу в фотоелектричних модулях, частково та повністю затемнена комірка та модуль.* Бібл. 21, табл. 6, рис. 7.
Ключові слова: **розміщення датчиків, виявлення та усунення несправностей, справна та несправна робота, фотоелектричне поле.**

Introduction. Photovoltaic (PV) market has been increased over the last years at a remarkable rate despite the economic difficulties. Worldwide photovoltaic energy production has surpassed 100 GW during the last decade reaching 138.9 GW in 2013 [1]. PV energy production becomes widely used because of its advantages as a renewable and clean energy source. It is eco-friendly, inexhaustible, easy to install, and the manufacturing time is relatively short. PV modules have a theoretical lifespan of approximately 20 years. In real-life and for several reasons, some PV modules start to fail after being used for a period of 8 to 10 years [2, 3]. Therefore, to ensure safe and reliable operation of PV power plants in a timely manner, a monitoring system must be established in order to detect, isolate and resolve faults.

The goal of the paper is the use of the bridge linked configuration to improve the performance of the photovoltaic field. The current of each string is measured continuously, however the voltage of each two successive modules and the overall voltage are measured only when the current of a string is reduced compared to the other strings. The photovoltaic generator operates at the maximum power point with the maximum power point tracking (MPPT) function regardless of the environmental effects.

Subject of investigations. This paper carries out a comprehensive study of the selection and the analysis of different topologies of sensors placement in the photovoltaic field. The conversion of solar radiation into DC occurs thanks to PV cell which represents the main component of PV array. One diode PV cell model shown in Fig. 1 is widely used regarding to its simplicity.

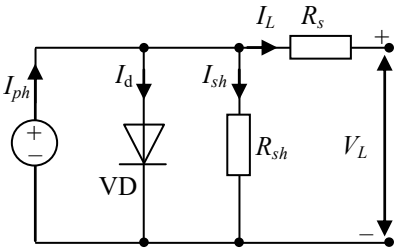

Fig. 1. One diode model of PV cell

Several electric models have been proposed to represent this model. PV cell is characterized by its characteristic current-voltage (I/V) which represent all its electrical configuration [4]. PV cell curve illustrated in Fig. 2 is defined by 3 essential variables: open circuit voltage (V_{oc}), short circuit current (I_{cc}) and maximum power point (MPP). Maximum power is obtained with an optimal voltage (V_{PPM}) and optimal current (I_{PPM}) [5, 6]. Operating the PV generator at its MPP is the role of MPP tracker.

The voltage generated by a PV cell is approximately 0.6 V. They should therefore be associated in series in modules [7, 8] (Fig. 3). The experimental results obtained from the 3 kinds of coupling series-parallel connection (SP), total cross tied connection (TCT), bridge linked

(BL) connection presented in [3], show that the TCT and BL wiring schemes have lower mismatch losses comparing to the SP structure leading to increase the power supplied by the PV field.

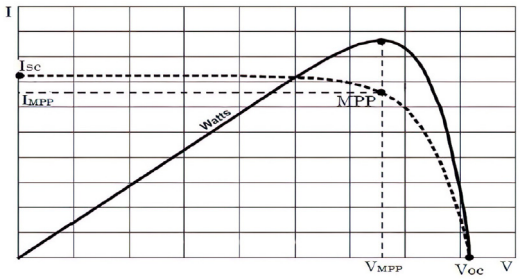

Fig. 2. Current-voltage (I/V) characteristic

In our case we are interested only in the BL configuration shown in Fig. 3,*f*. This topology reduces the number of connections between the modules by about half compared to the TCT topology, which significantly reduces the amount deducted and the length of the wiring of the PV array.

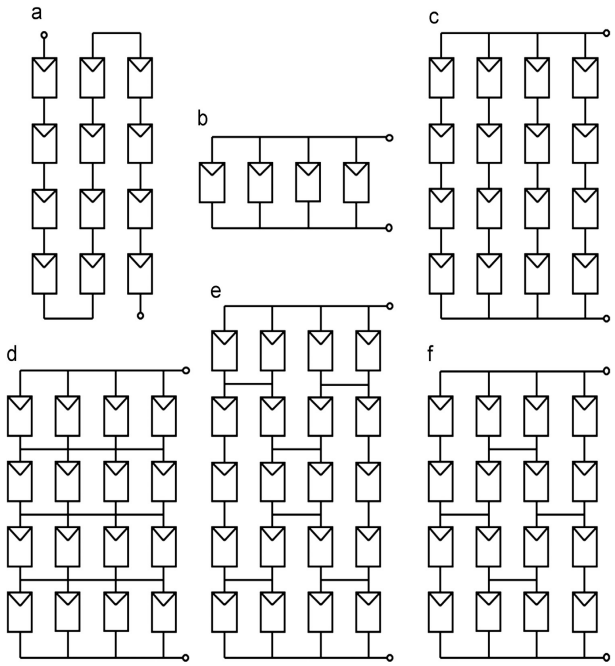

Fig. 3. Main interconnection models of PV modules: (*a*) serial connection, (*b*) parallel connection, (*c*) series-parallel connection (SP), (*d*) total cross tied connection (TCT), (*e*) honey-comb connection (HC), (*f*) bridge linked connection (BL)

Faults detection and isolation. The process of voltage and current sensors placement is illustrated in Fig. 4. One voltage sensor is placed for two successes PV modules linked by node and one current sensor is placed at the end of each string. For each field (M, N), N current sensors and $[(N–1)\cdot(N+1)/2]$ voltage sensors are needed. If $[(N–1)\cdot(N+1)]$ is odd we use the integer number for voltage sensors which use (m, n) label as follows.

This new model allows detection and isolation of the faults by comparing the following measured quantities:

- the current of each string (I_1 ... I_M);
- the overall output voltage U;
- the voltage of 2 successive modules connected by a node U_{mn}.

By this way, the string fault can be detected by current analysis of all strings and accurately locate the fault according to U_{mn}. In the healthy operating state, the currents of each string in the same PV modules number are identical and the voltages of each two successive modules linked by node are identical.

Different topologies of connecting PV modules. Like it is shown in Fig. 3, several PV module's interconnection topologies are proposed in the literature [9, 10].

Different types of faults. The main type faults and their causes are detailed in Table 1 [2].

Table 1

Categories of faults

Types of faults		Causes
Module damage (aging)		Increase of the series resistor R_s. Decrease in shunt resistor R_{sh}. Deterioration of the antireflection layer of the cell.
Short circuit	Cell	This failure easily occurs in thin film cells because the top and bottom electrodes are much closer together.
	Module	Resulting faults in the manufacturing process.
Open circuit	Cell	Fragmentation of cells
	Module	Loose wires
Hot point		Partial and total shading

Method for voltage and current measurement. The collection of measured values using current and voltage sensors at different points of the PV field allows to detect precisely the fault and to isolate it through comparison of these measures with nominal data. A brief summary of literature works in this context is presented in Table 2. According to authors in Table 2, voltage and current measurement methods focus on two axes:

a) methods designed for TCT coupling;

b) the proposed methods for SP coupling.

The following methods can be cited as follow.

Methods of voltage measurement. This method is described by authors in Table 2.

Table 2

Methods of voltage measurement proposed in the literature

Methods of voltage and current measurement		
Types of coupling	Reference	Analysis
Total cross tied (TCT) connection	[11, 12]	This model is used for coupling. In each string is placed one voltage sensor for measurement with parallel connection. Each string is subdivided into group which use current sensor.
Series-parallel (SP) connection	[13, 14]	This sensor placement model is used for PV field connected series-parallel. Each bloc can present one group of PV modules with current sensor. The faults position can be located by analyzing the current and voltage variation of each branch.

Method of an infrared imaging. The faults in PV array can be precisely located using a thermal camera [15].

Method of operating point analyzing. This method is based on analysis and comparison of the current with the expected MPP [16].

Other methods. In [17], authors used artificial neural networks analysis and in [18] and [19], fuzzy control theory is used for diagnosis.

New voltage and current measurement method. This new method is adapted to the BL configuration. Fault points can be detected and isolated quickly and accurately by comparing the measured values. Considering that a PV array consists of N strings containing M modules per string, we can determine $[(M–1)\cdot(N–1)/2)]$ connections (if $(M–1)\cdot(N–1)$ is an odd integer is used $[(M–1)\cdot(N–1)/2])$. The connection is labeled (m, n) if it is located below and to the right of the (m, n) module [18, 20, 21].

Sensor's placement technique. In this case, a voltage sensor is placed for two successive modules connected by a node, and a current sensor is placed at the end of each string as illustrated in Fig. 4. Then a field for (M, N) needs N current sensors and $[(M–1)\cdot(N+1)/2]$ voltage sensors (if $(M–1)\cdot(N+1)$ is an odd integer is used $[(M–1)\cdot(N+1)/2]$). Each voltage sensor takes the label (m, n) with:

$$\begin{cases} N: pair \begin{cases} m = 1...M-1. \\ n = (2k) - (1 - m \bmod 2). \end{cases} \\ where: \begin{cases} k = 1....N/2 (m: pair). \\ k = 1....(N/2)+1 (m: impair). \end{cases} \end{cases} \quad (1)$$

$$\begin{cases} N: impair \begin{cases} m = 1...M-1. \\ n = (2k) - (1 - m \bmod 2). \end{cases} \\ where: k = 1...(N+1)/2. \end{cases} \quad (2)$$

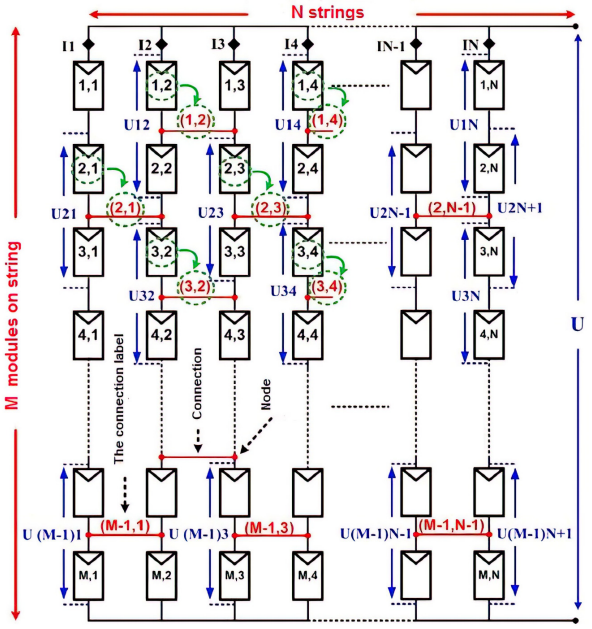

Fig. 4. New sensor placement scheme in PV array

Faults diagnosis principle. This new fault diagnosis model is used to isolate the detected fault point by comparing the following measured quantities:

The current of each string (I_1 ... I_M), the overall output voltage U and the voltage of two successive modules connected by a node U_{mn}. The thong fault can be detected by current analysis of all the strings and precise location of the fault can be localized according U_{mn}.

In healthy operating state, the current of each string to identical number of PV modules is the same. Thus, the fault in a string is confirmed if the current is dropped compared to another healthy string.

A criterion I_S (standard current) is specified to distinguish between real faults and small perturbations.

For example, in a (3, 3) PV array as it is shown in Fig. 5, this criterion is given by:

$I_S = 90\%\ I_{max}$, where $I_{max} = \max\{I_1, I_2, .., I_M\}$.

If the first string is supposed to be faulty, then $I_1 < I_S$, and the standard current $I_S = 90\% I_{max}$, where $I_{max} = \max(I_2, I_3)$.

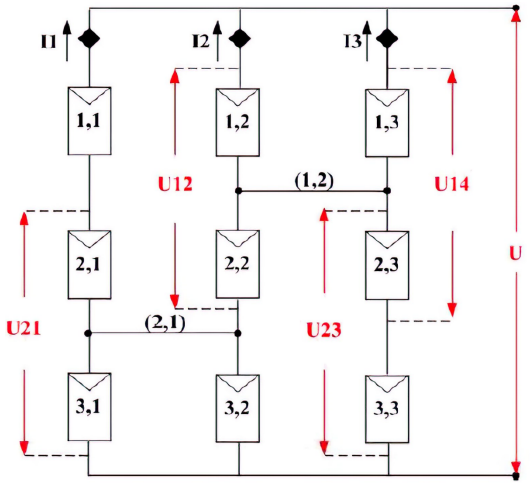

Fig. 5. (3, 3) PV array

- U_{12} and U_{21} are the voltage values of the first faulty string.
- U_{12} and U_{23} are the voltage values of the second faulty string.
- U_{14} and U_{23} are the voltage values of the third faulty string.
- $U_S = 2/3U$ is the standard voltage.

The result between U_{12}, U_{21} and U_S allows locating the faults in the faulty string.

Three cases are possible:

$$\begin{cases} \text{if } U_{12} < U_S, U_{21} > U_S \text{ and } I_1 < I_S \text{ then module}(1,1) \text{ is faulty,} \\ \text{if } U_{12} < U_S, U_{21} < U_S \text{ and } I_1 < I_S \text{ then module}(2,1) \text{ is faulty;} \\ \text{if } U_{12} > U_S, U_{21} < U_S \text{ and } I_1 < I_S \text{ then module}(3,1) \text{ is faulty.} \end{cases} \quad (3)$$

According to this criterion, a fault in the string is determined if the current is less than the standard current I_S when the faulty state is not confirmed.

The voltage U_{mn} of two successive modules connected by one node is identical to the healthy operating state and vice versa.

After determining the k^{th} faulty string, the fault point location in this string is located in function of its voltage.

The values of i and j are given by the following relationship:

$$\begin{cases} i = 1...M-1. \\ j = k + i \bmod 2 (k: impair) \\ j = k + 1 - i \bmod 2 (k: pair). \end{cases} \quad (4)$$

The criterion for a fault point location is $U_S = 2U/M$, where U is the output voltage of the PV field; M is the number of modules per string. When U_{ij} exceeds U_S, it means that there is no fault in these 2 modules. Finally, the fault point will be located after the comparison between each voltage of U_{ij} and U_S.

Faults detection and isolation algorithm. The algorithm of the faults detection and isolation (FDI) is illustrated in Fig. 6.

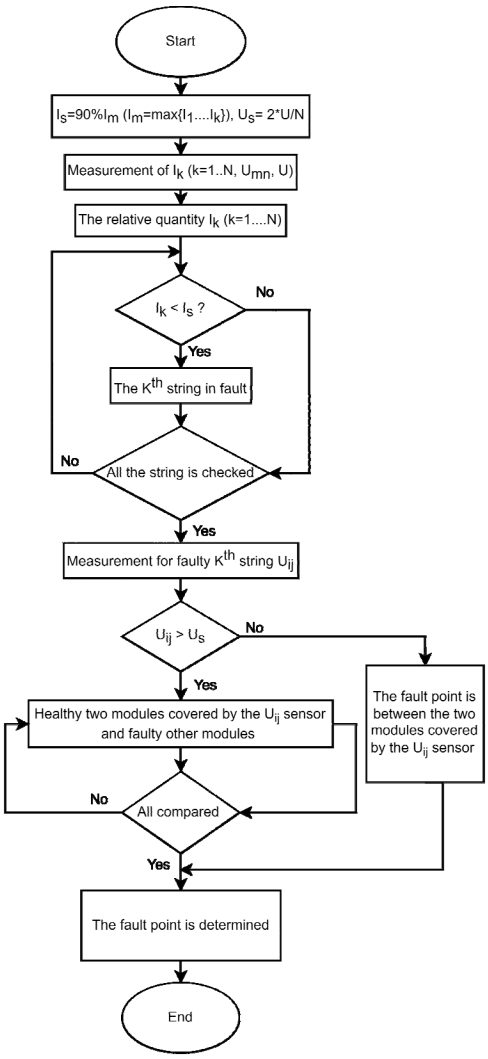

Fig. 6. FDI algorithm

Simulation results. The feasibility of the sensor placement model proposed in this work is proven by simulation results under MATLAB/Simulink environment for several types of defects.

The PV module used in this simulation is «Solarex MSX-60» with 36 cells in series. The electrical characteristics are represented in Table 3.

The criterion of the selection of the standard current is specified in order to distinguish between the real fault and the perturbations.

If the current decreases less than 10 % of the nominal current then no fault was detected because this situation cannot be dysfunction the model.

This criterion explains how the 90 % threshold was chosen to distinguish a defective string from the string with a maximum current.

The simulated model contains 9 (3, 3) modules (Fig. 7). 5 voltage sensors and 3 current sensors have to be placed.

The simulation is carried out under standard conditions (solar irradiance is 1000W/m², atmospheric mass is 1.5 and cell temperature is 25°C.

The BL configuration illustrated by Fig. 7 in the paper with sensors placement is realized under MATLAB/Simulink and after simulation of this model we obtained the results of 3 scenario of Table 4 and 5. This model can be realized in real time with more material tool which is not available at our laboratory.

The simulation parameters of the module are chosen as follows: serial resistor R_S = 0.23 **Ω**, parallel resistor R_{SH} = 6720.65 **Ω**, photo-current I_{ph} = 3.81 A and ideality factor n = 1.29. In the simulation the module faults (disconnected, short-circuited) and shadow faults (hot point phenomenon) are considered.

Three different scenarios can be proposed: the module is disconnected (scenario 1); short-circuited cell, several short-circuited cells, short-circuited module (scenario 2) and different levels of shading (scenario 3).

Table 3

Methods of voltage measurement proposed in literature

Faulty strings	String 1			String 2			String 3		
Standard current I_S	90% max(I_2, I_3)			90% max(I_1, I_3)			90% max(I_1, I_2)		
Faulty string current	$I_1<I_S$			$I_2<I_S$			$I_3<I_S$		
Faulty module	(1, 1)	(2, 1)	(3, 1)	(1, 2)	(2, 2)	(3, 2)	(1, 3)	(2, 3)	(3, 3)
Standard voltage U_S	(2/3)U			(2/3)U			(2/3)U		
Voltage of two successive modules with faulty string	$U_{12}<U_S$ $U_{21}>U_S$	$U_{12}<U_S$ $U_{21}<U_S$	$U_{12}>U_S$ $U_{21}<U_S$	$U_{13}<U_S$ $U_{23}>U_S$	$U_{13}<U_S$ $U_{23}<U_S$	$U_{13}>U_S$ $U_{23}<U_S$	$U_{14}<U_S$ $U_{24}>U_S$	$U_{14}<U_S$ $U_{24}<U_S$	$U_{14}>U_S$ $U_{24}<U_S$

First scenario. In this scenario, we disconnect a string of modules. All other elements of the field are in normal conditions. From the results of Table 4, the open-circuit fault is confirmed due to the zero value of the first-string current of PV array.

The faulty module number is limited between (1, 1) and (2, 1) as U_{12} < 2/3U, but the (2, 1) module is confirmed flawless because U_{21} value is greater than 2/3U, this analysis can confirm that there is an open-circuit fault at the module level (1, 1).

Second scenario. In this scenario, three faulty states are treated: a shorted cell, a group of short-circuited cells (18 cells) and a short-circuited module (36 cells at a time).

According to the results in Table 4, the output current and voltage decreased due to the short circuit fault. It is found that the faultier cells increase over the current and voltage also decreases.

However, the operating state is almost the same as the healthy state when the fault occurred at a single cell, because of this small decrease cannot confirm whether a default has occurred or not at installation.

The standard current I_S is equal to 90 % $I_{\max}$ with $I_{\max}$ = max {I_1, I_2, I_3}. According to this criterion, the fault is confirmed in the system when a group of 18 cells (82.7 % I_1 = I_2) or when a module is completely shorted (I_1 I_2 = 80 %). In both cases the current string in fault I_1 is less than I_S. On to less than 2/3U, U_{12} and U_{21} voltages are higher than 2/3U, so the fault is located at the module level (1, 1).

Third scenario. In this scenario, different shading rates are applied on a cell module covering the cell partially and completely. Shading of the PV cell greatly affects the power output of the plant.

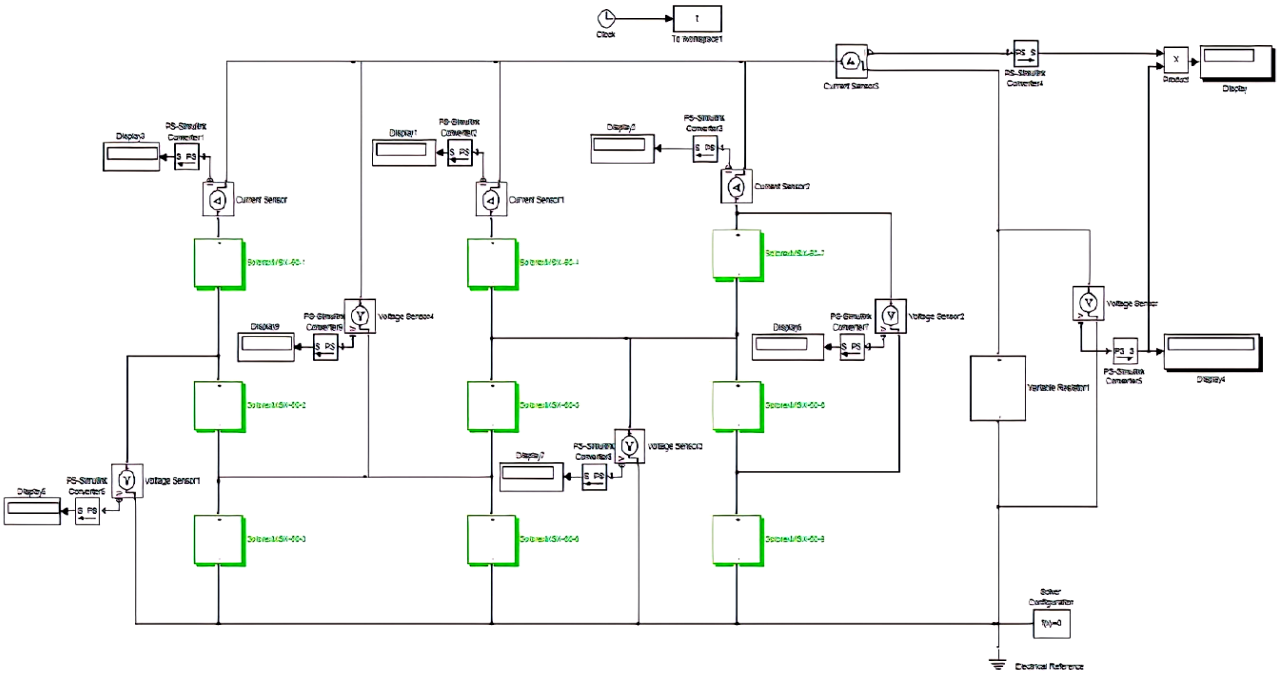

Fig. 7. The simulated model under Matlab/Simulink environment

Table 4

Scenarios 1 and 2

	Normal state	Scenario 1	Scenario 2		
		Open circuit	1 cell	18 cells	36 Cells
I_1	3.54	0	3.52	3.12	3.04
I_2	3.54	3.57	3.56	3.77	3.80
I_3	3.54	3.57	3.56	3.77	3.80
U_{12}	34.03	32.25	33.81	27.41	18.43
U_{21}	34.03	40.91	34.17	35.65	35.95
U_{14}	34.03	34.49	33.88	29.64	23.69
U_{23}	34.03	35.17	33.91	30.30	24.51
$2/3U$	34.03	34	33.88	29.86	23.96

Table 5

Scenario 3

	Normal state	Scenario 3			
		1 cell shaded at 10 %	1 cell shaded at 30 %	1 cell shaded at 50%	1 cell shaded at 100 %
I_1	3.54				
I_2	3.54				
I_3	3.54				
U_{12}	34.03	34.59			
U_{21}	34.03	34.38	34.2	34.29	33.83
U_{14}	34.03	34.47	35.06	34.63	36.25
U_{23}	34.03	34.41	34.42	34.6	34.28
$2/3U$	34.03	34.17	34.84	35.28	35.6

According to the results of Table 5, the power is reduced to 29 % of the real value when PV cell is completely shaded.

When the shaded area of the cell is less than or equal to 50 % of the total area, the fault cannot be confirmed because of the value of the current I_1 fault string exceeds I_S ($I_1 > I_2$ 90 %).

In the case when a cell in a PV module is completely shaded, 83 % $I_1 = I_2$, then the fault is confirmed. Because of the value of U_{12} is greater than $2/3U$ and U_{21} is less than $2/3U$, I_S is produced at the module level (3, 1).

The comparison between SP and BL configurations can be summarized in Table 6.

Table 6

Results of SP and BL configurations

	Normal state		Open circuit	
	SP	BL	SP	BL
I_1, A	6.79	3.54	0	0
I_2, A	6.79	3.54	6.87	3.57
I_3, A	6.79	3.54	6.87	3.57
U_{12}, V	54.99	34.03	42.95	32.25
U_{21}, V	54.99	34.03	65.80	40.91

The voltage in the faulty string of BL configuration is less than the voltage in SP configuration.

Conclusions.

In this paper, a new sensor placement combination for the detection and isolation of faults in the photovoltaic field and the simulation results for different types of faults are presented.

The number of sensors required and the costs are reduced significantly in this model compared to other existing models.

The faults detection and isolation method developed in this work is confirmed by three different scenarios by showing how different faults affecting the photovoltaic field such as short-circuit current, open circuit voltage, partial and total shading can be presented.

This study opens many perspectives:

- applying this method to the real photovoltaic field;
- applying one structure for faults identification;
- for the diagnostic multi faults cumulated can be expected.

Acknowledgement. The authors would like to thank Monitoring Team of Automation Laboratory – LAS, University of Setif 1, Setif, Algeria.

Conflict of interest. The authors declare that they have no conflicts of interest

REFERENCES

1. European Photovoltaic Industry Association (EPIA). *Global Market Outlook for Photovoltaics 2014-2018*. Available at: https://helapco.gr/wp-content/uploads/EPIA_Global_Market_Outlook_for_Photovoltaics_2014-2018_Medium_Res.pdf (accessed 16 May 2021).

2. Al-Sheikh H., Moubayed N. Fault detection and diagnosis of renewable energy systems: An overview. *2012 International Conference on Renewable Energies for Developing Countries (REDEC)*, 2012, pp. 1-7. doi: https://doi.org/10.1109/REDEC.2012.6416687.

3. Sholapur S., Mohan K.R., Narsimhegowda T.R. Boost Converter Topology for PV System with Perturb And Observe MPPT Algorithm. *IOSR Journal of Electrical and Electronics Engineering*, 2014, vol. 9, no. 4, pp. 50-56. doi: https://doi.org/10.9790/1676-09425056.

4. Ghazanfari J., Maghfoori Farsangi M. Maximum Power Point Tracking Using Sliding Mode Control for Photovoltaic Array. *Iranian Journal of Electrical and Electronic Engineering*, 2013, vol. 9, no. 3, pp. 189-196. Available at: http://ijeee.iust.ac.ir/article-1-523-en.pdf (accessed 16 May 2021).

5. Latreche S., Badoud A.E., Khemliche M. Implementation of MPPT Algorithm and Supervision of Shading on Photovoltaic Module. *Engineering, Technology & Applied Science Research*, 2018, vol. 8, no. 6, pp. 3541-3544. doi: https://doi.org/10.48084/etasr.2354.

6. Nebti K., Lebied R. Fuzzy maximum power point tracking compared to sliding mode technique for photovoltaic systems based on DC-DC boost converter. *Electrical Engineering & Electromechanics*, 2021, no. 1, pp. 67-73. doi: https://doi.org/10.20998/2074-272X.2021.1.10.

7. Levron Y., Shmilovitz D. Maximum Power Point Tracking Employing Sliding Mode Control. *IEEE Transactions on Circuits and Systems I: Regular Papers*, 2013, vol. 60, no. 3, pp. 724-732. doi: https://doi.org/10.1109/TCSI.2012.2215760.

8. Meng Z., Shao W., Tang J., Zhou H. Sliding-mode control based on index control law for MPPT in photovoltaic systems. *CES Transactions on Electrical Machines and Systems*, 2018, vol. 2, no. 3, pp. 303-311. doi: https://doi.org/10.30941/CESTEMS.2018.00038.

9. Picault D. *Reduction of mismatch losses in grid-connected photovoltaic systems using alternative topologies*. Sciences de l'ingénieur [physics]. Institut National Polytechnique de Grenoble, 2010. France. Available at: https://tel.archives-ouvertes.fr/file/index/docid/545432/filename/Thesis_dpicault.pdf (accessed 16 May 2021).

10. La Manna D., Li Vigni V., Riva Sanseverino E., Di Dio V., Romano P. Reconfigurable electrical interconnection strategies for photovoltaic arrays: A review. *Renewable and Sustainable Energy Reviews*, 2014, vol. 33, pp. 412-426. doi: https://doi.org/10.1016/j.rser.2014.01.070.

11. Yanli Liu, Bingfeng Li, Ze Cheng. Research on PV module structure based on fault detection. *2010 Chinese Control and Decision Conference*, 2010, pp. 3891-3895. doi: https://doi.org/10.1109/CCDC.2010.5498470.

12. Xu X., Wang H., Xu X., Zuo Y. Method for Diagnosing Photovoltaic Array Fault in Solar Photovoltaic System. *2011 Asia-Pacific Power and Energy Engineering Conference*, 2011, pp. 1-5. doi: https://doi.org/10.1109/APPEEC.2011.5747701.

13. Huang Zhiqiang, Guo Li. Research and implementation of microcomputer online fault detection of solar array. *2009 4th International Conference on Computer Science & Education*, 2009, pp. 1052-1055. doi: https://doi.org/10.1109/ICCSE.2009.5228541.

14. Jianeng T., Yongqiang Z., Wenshan W. Fault diagnosis method and simulation analysis for photovoltaic array. *2011 International Conference on Electrical and Control Engineering*, 2011, pp. 1569-1573. doi: https://doi.org/10.1109/ICECENG.2011.6058271.

15. Schirripa Spagnolo G., Del Vecchio P., Makary G., Papalillo D., Martocchia A. A review of IR thermography applied to PV systems. *2012 11th International Conference on Environment and Electrical Engineering*, 2012, pp. 879-884. doi: https://doi.org/10.1109/EEEIC.2012.6221500.

16. Chouder A., Silvestre S. Automatic supervision and fault detection of PV systems based on power losses analysis. *Energy Conversion and Management*, 2010, vol. 51, no. 10, pp. 1929-1937. doi: https://doi.org/10.1016/j.enconman.2010.02.025.

17. Syafaruddin, Karatepe E., Hiyama T. Controlling of artificial neural network for fault diagnosis of photovoltaic array. *2011 16th International Conference on Intelligent System Applications to Power Systems*, 2011, pp. 1-6. doi: https://doi.org/10.1109/ISAP.2011.6082219.

18. Cheng Z., Zhong D., Li B., Liu Y. Research on Fault Detection of PV Array Based on Data Fusion and Fuzzy Mathematics. *2011 Asia-Pacific Power and Energy Engineering Conference*, 2011, pp. 1-4. doi: https://doi.org/10.1109/APPEEC.2011.5749018.

19. Mahmoud S.A., Mohamed H.N. Novel modeling approach for photovoltaic arrays. *2012 IEEE 55th International Midwest Symposium on Circuits and Systems (MWSCAS)*, 2012, pp. 790-793. doi: https://doi.org/10.1109/MWSCAS.2012.6292139.

20. Alajmi B.N. *Design and Control of Photovoltaic Systems in Distributed Generation*. Thesis for the degree of Doctor of Philosophy, University of Strathclyde, Department of Electronic and Electrical Engineering. 2013. Available at: https://stax.strath.ac.uk/downloads/gt54kn312 (accessed 16 May 2021).

21. Khan S.A., Mahmood T., Awan K.S. A nature based novel maximum power point tracking algorithm for partial shading conditions. *Electrical Engineering & Electromechanics*, 2021, no. 6, pp. 54-63. doi: https://doi.org/10.20998/2074-272X.2021.6.08.

Received 23.03.2022
Accepted 15.06.2022
Published 07.09.2022

Latreche Samia[1], *Doctor of Technical Science, Associate Professor,*
Khenfer Amar[1], *PhD Student,*
Khemliche Mabrouk[1], *Doctor of Technical Science, Professor,*
[1] Technology Faculty, Electrical Engineering Department, Automation Laboratory of Setif, University of Setif 1, Algeria.
e-mail: ksamia2002@yahoo.fr (Corresponding Author), khenferamar@yahoo.fr, mabroukkhemliche@univ-setif.dz

How to cite this article:
Latreche S., Khenfer A., Khemliche M. Sensors placement for the faults detection and isolation based on bridge linked configuration of photovoltaic array. *Electrical Engineering & Electromechanics*, 2022, no. 5, pp. 41-46. doi: https://doi.org/10.20998/2074-272X.2022.5.07